*Proc. 15th Int. Symp. Origin of Matter and Evolution of Galaxies (OMEG15)*
JPS Conf. Proc. **31**, 011032 (2020)
https://doi.org/10.7566/JPSCP.31.011032

# *s*-process Nucleosynthesis in AGB Stars at Low-Metallicity

Takuma SUDA[1,2], Shimako YAMADA[3] and Masayuki Y. FUJIMOTO[3]

[1] *The Open University of Japan, Wakaba 2-11, Mihama-ku, Chiba, Chiba 261-8586, Japan*
[2] *Research Center for The Early Universe, University of Tokyo, Hongo 7-3-1, Bunkyo-ku, Tokyo 113-0033, Japan*
[3] *Faculty of Science, Hokkaido University, Kita 10 Nishi 8, Kita-ku, Sapporo, Hokkaido 060-0810, Japan*

*E-mail: suda@resceu.s.u-tokyo.ac.jp*

(Received November 7, 2019)

The first stars in the universe must have provided chemical imprints in the surface of observed metal-poor stars with [Fe/H]$\lesssim -2$. One of the most important signatures is the abundances of carbon-enhanced metal-poor (CEMP) stars, which are defined as [C/Fe] $\geq 0.7$. The origins of CEMP stars and its subclasses such as CEMP-*s* and CEMP-no stars, divided by the enhancement of *s*-process elements, engage the keenest attention of those who working on first stars and stellar archaeology. However, in spite of the obvious importance of the role of the *s*-process in AGB stars at low-metallicity, theoretical models and their applications to CEMP stars with [Fe/H] $\lesssim -2.5$ are not well investigated, while it is established that metal-poor AGB stars undergo a proton ingestion episode that triggers the *s*-process. In this paper, three modes of the *s*-process, the convective $^{13}$C burning triggered by the proton ingestion episode, the convective $^{22}$Ne burning, and the radiative $^{13}$C burning, are considered, using a detailed nucleosynthesis code customized to compute the *s*-process in metal-poor AGB stars. We argue that neutron exposure is dominated by oxygen abundance, not by iron abundance, at metallicity below [Fe/H] $\sim -2$. Based on this discovery, we provide a comprehensive understanding of the *s*-process in EMP AGB stars, together with the connection to the observations.

**KEYWORDS:** stellar evolution, nucleosynthesis, AGB stars, metal-poor stars

## 1. Introduction

Extremely metal-poor (EMP) stars, whose typical metallicities are [Fe/H] $\lesssim -3$, are important tracers of star formation history in the early universe. Among them, carbon-enhanced metal-poor (CEMP) stars provide useful information on the evolution of metal-poor stars, having the iron abundance of [Fe/H] $\lesssim -2$. They comprise at least more than 10 % of the known metal-poor stars [1], and have a key to our understanding of nucleosynthesis in metal-poor environment.

There have been an argument on the classification of CEMP stars into several subgroups (see, e.g. [2,3]). The most well accepted and common populations are CEMP-*s* and CEMP-no stars, which stands for *s*-process-rich and Ba-normal, respectively. Abundance analyses with high-resolution spectroscopy have revealed that CEMP-no stars dominate the population at [Fe/H] $\lesssim -3$ [4].

The origin of CEMP-no stars is still in controversy, whether CEMP-*s* and CEMP-no stars share the common origin in terms of nucleosynthesis. In particular, the source of carbon in CEMP stars are the major concern regarding the origins of the most iron-poor stars. It is to be noted that long-term monitoring of radial velocities for CEMP-no stars, including the hyper metal-poor star, HE 0107-5240, has increased the fraction of binaries among them [5], suggesting that a binary mass transfer can be responsible for carbon and/or *s*-process elements in CEMP-no stars. Observationally, the distribution of [Ba/C] as a function of metallicity is continuous rather than discrete between CEMP-*s* and CEMP-no stars as shown in Figure 1, which implies that CEMP-*s* and CEMP-no stars

have the same origin. In the figure, CEMP-no stars show smaller carbon enhancement than CEMP-s stars, whatever the trend of carbon abundance is. This also implies that CEMP-no stars belong to longer periond binaries if the amount of C dredged-up to the surface in AGB stars is constant.

These can be interpreted that CEMP-no stars should also have or had binary companions since it is almost established that the abundances of CEMP-*s* stars are the result of binary mass transfer events. It is expected that C and *s*-process elements are transported together during the binary mass transfer, because these elements are synthesized in the helium burning layers, dredged-up to the surface in a primary star, and transferred to a secondary star, keeping the abundance ratio constant.

On the other hand, there is an outlier for the [Ba/C] in the figure. Apparently the efficiency of the *s*-process is lower than other CEMP stars. In this paper, we separate the CEMP-no stars by the lower dashed line in Fig. 2 ([Ba/C] = [Fe/H] + 0.8) and name them Hi-CEMP-no and Lo-CEMP-no stars.

In this study, we explore the *s*-process nucleosynthesis in AGB stars by assuming that the binary mass transfer scenario [6] applies to all the CEMP stars. We compute the *s*-process in EMP AGB stars to provide a general picture of the origin of CEMP stars.

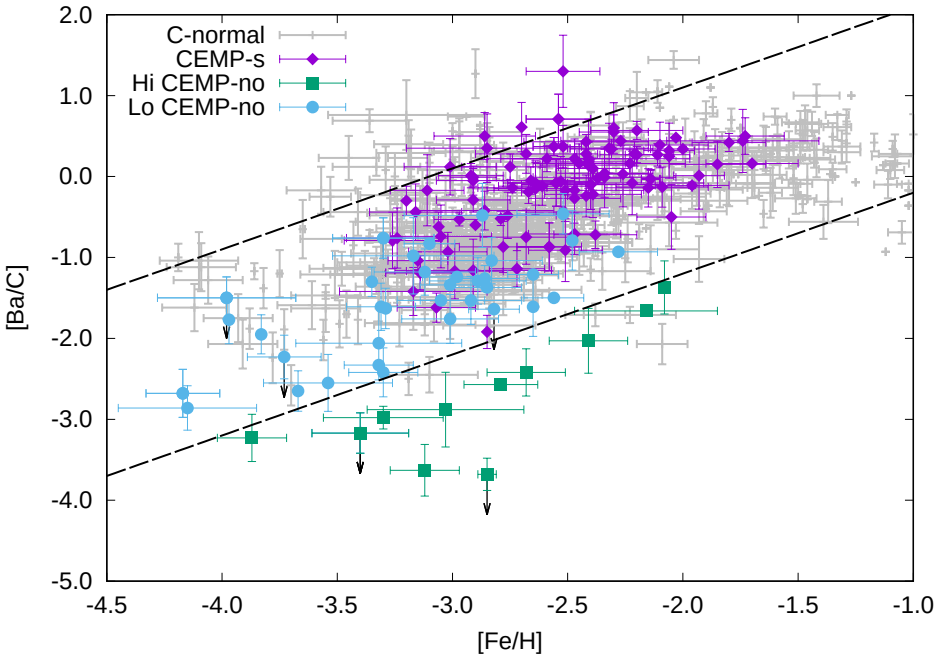


**Fig. 1.** The abundance ratio of barium to carbon as a function of metallicity. The two dashed lines ([Ba/C] = [Fe/H] + 3.1 and [Ba/C] = [Fe/H] + 0.8) represent the possible efficiency of the *s*-process in AGB stars, inferred from the location occupied by CEMP-*s* stars. The data are taken from the SAGA database [7–10]

## 2. Models

Three modes of the *s*-process nucleosynthesis in EMP AGB stars are considered: (1) C13C mode: the convective $^{13}$C burning which is triggered by the hydrogen mixing into the helium-flash convective zones [6, 14–16], (2) C22Ne mode: the convective $^{22}$Ne burning which is the *s*-process in the helium-flash convective zones with a neutron source from $^{22}\mathrm{Ne}\,(\alpha, n)^{25}\,\mathrm{Mg}$ [18], and (3) R13C pocket mode: the radiative $^{13}$C pocket which is triggered by the hydrogen mixing at the bottom of the envelope during the third dredge-up.

We use the nuclear network code [11], based on one-zone approximation, following the time evolution of the temperature of the nucleosynthesis site during the helium shell flashes [12]. We have extended the nuclear network code by including more than 300 isotopes with proton-, $\alpha$-, and neutron-capture reactions and $\beta$-decays.

The hydrogen mixing events are controlled by the parameters to fix the amount of mixed $^{13}$C and the timescale of mixing. Stellar models are taken from the results of one-dimensional stellar models [14, 16]. The details of the models and parameters are described in [20].

## 3. Results

The *s*-process nucleosynthesis differs greatly at [Fe/H] $\lesssim -2$ in our models. This critical metallicity reflects the efficiency of the absroption of neutrons by $^{16}$O and $^{17}$O rather than the iron group elements. Around the critical metallicity, there are three stages of the *s*-process, by increasing the neutron density, i.e., the amount of mixing. The first stage of the *s*-process is the absorption of neutrons by the iron group elements, where neutrons are produced by $^{13}\mathrm{C}\,(\alpha, n)^{16}\mathrm{O}$ in the helium burning shell. This produces heavy elements up to Bi and Pb. The second stage of the *s*-process is the neutron absorption by oxygen isotopes when all the iron-group elements contained initially in the helium burning shell are used to synthesize heavy *s*-process elements. At this stage, the production efficiency of *s*-process elements decreases because oxygen works as a neutron poison. It is to be noted that $^{12}$C is the most efficient absorber of neutrons, but it emits a neutron by the neutron recycling reactions [11, 13]. The third stage of the *s*-process is the recovery of *s*-process nucleosynthesis by the production of the iron-group elements from neon and magnesium isotopes by the accumulation of light elements by the neutron- and $\alpha$-capture reactions of oxygen isotopes.

Our analysis shows that the *s*-process is mainly controlled by oxygen and not by iron below the critical metallicity. In our simulations, the final abundance distribution of the *s*-process elements is independent of metallicity at [Fe/H] $\lesssim -2$. It is generally thought that neutron per seed nuclei increases with decreasing metallicity at [Fe/H] $\geq -2.5$, which leads to the more efficient production of heavy-*s* elements [19], while it is not the case at very low metallicity.

Figure 2 shows the comparison of our models with the observations of CEMP stars taken from the SAGA database. This diagram provides the useful comparison because the variation in [Ba/C] is indepedent of binary parameters. The colored areas shows the final abundances covered by changing the model parameters. It is clear that the convective $^{13}$C burning in metal-poor AGB stars (left panel) cover all the observed values, irrespective of CEMP-*s* or CEMP-no. The coverage of the C22Ne mode (center) is smaller than the C13C mode, but this process reasonably covers the domain of Hi-CEMP-no stars. The R13C pocket (right) mode plays the least role among the three modes of the *s*-process. In particular, the size of the $^{13}$C pocket is, in general, too small to produce *s*-process elements sufficient to explain the observed values of [Ba/C].

## 4. Discussions

We have computed the *s*-process nucleosynthesis in AGB stars to reproduce the observed abundances of carbon-enhanced metal-poor stars with and without the enhancement of *s*-process elmements (CEMP-*s* and CEMP-no, respectively), which explores the possibility of the binary mass transfer scenario. We find that the abundance patterns of CEMP-no stars are explained by the binary scenario.

The result gives an insight into binary star formation in the early universe. Our previous studies demonstrated that the initial mass function (IMF) changed at the critical metallicity of [Fe/H] $\sim -2$ [17]. Below this critical metallicity, it is suggested that another critical metallicity may exist at [Fe/H] $\sim -3.5$, below which only the progenitors of Lo-CEMP-no stars are formed. CEMP-*s*

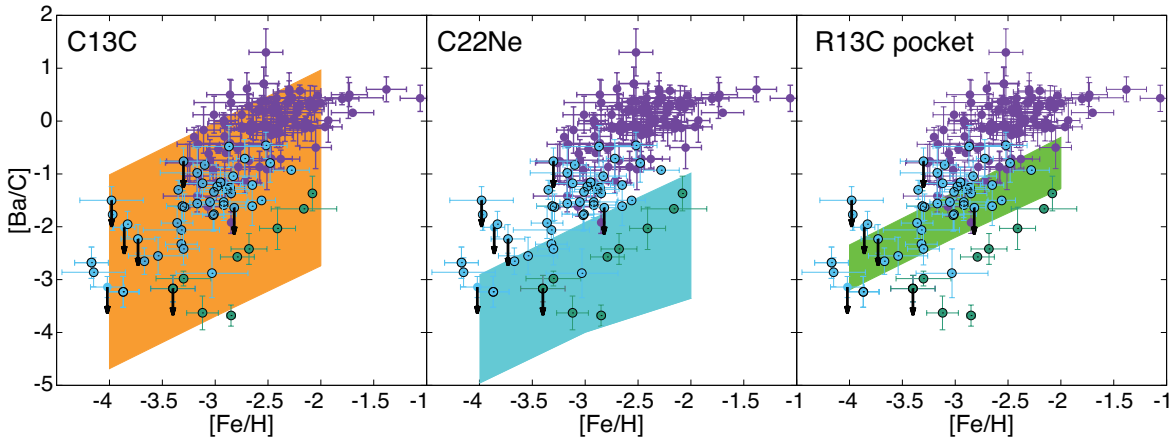


**Fig. 2.** Comparison of models with the observations of CEMP stars. The hatched area on the left, in the center, and on the right is the region covered by the parameters of the *s*-process in our AGB models, where the neutron source is the $\alpha$-capture of $^{13}$C, $^{22}$Ne, and the radiative $^{13}$C pockect, respectively. The meanings of the symbols are the same as in Fig. 1.

and Hi-CEMP-no stars should not be formed at [Fe/H] $\lesssim -3.5$ from the comparison between our theoretical models and the observations. This is equivalent to the formation of low-mass stars with the companions of intermediate-mass stars that produce *s*-process elements during the AGB phase.

More detailed discussion will be given in a separate paper [20].

## Acknowledgement

This work has been supported by JSPS KAKENHI Grant Number 16H02168 and 16K05287.

## References

[1] J. E. Norris and D. Yong, Astrophys. J., **879**, 37, (2019).
[2] P. Bonifactio *et al.*, Astron. Astr., **579**, A28, (2015).
[3] J. Yoon *et al.*, Astrophys. J., **833**, 20, (2016).
[4] W. Aoki, *et al.*, Astrophys. J., **655**, 492, (2007).
[5] A. Arentsen, E. Starkenburg, M. D. Shetrone, K. A. Venn, É. Depagne, and A. W. McConnachie, Astron. Astr., **621**, A108, (2019).
[6] T. Suda, M. Aikawa, M. N. Machida, M. Y. Fujimoto and I. Iben Jr., Astrophys. J., **611**, 476, (2004).
[7] T. Suda *et al.*, Publ. Astron. Soc. Jpn., **60**, 1159, (2008).
[8] T. Suda *et al.*, Mon. Not. R. Astron. Soc., **412**, 843, (2011).
[9] S. Yamada, T. Suda, Y. Komiya, W. Aoki, and M. Y. Fujimoto, Mon. Not. R. Astron. Soc., **436**, 1362, (2013).
[10] T. Suda *et al.*, Publ. Astron. Soc. Jpn., **69**, 76, (2017).
[11] T. Nishimura, M. Aikawa, T. Suda, and M. Y. Fujimoto, Publ. Astron. Soc. Jpn., **61**, 909, (2009).
[12] M. Aikawa, M. Y. Fujimoto, K. Kato, Astrophys. J., **560**, 937, (2001).
[13] R. Gallino, M. Busso, G. Picchio, C. M. Raiteri, and A. Renzini, Astrophys. J., **334**, L45, (1988).
[14] M. Y. Fujimoto, Y. Ikeda, and I. Iben Jr., Astrophys. J., **529**, L25, (2000).
[15] S. W. Campbell and J. C. Lattanzio, Astron. Astr. **490**, 769, (2008).
[16] T. Suda and M. Y. Fujimoto, Mon. Not. R. Astron. Soc., **405**, 177, (2010).
[17] T. Suda *et al.*, Mon. Not. R. Astron. Soc., **432**, L46, (2013).
[18] M. Lugaro, A. I. Karakas, R. J. Stancliffe, and C. Rijs, Astrophys. J., **747**, 2, (2012).
[19] A. Karakas and J. C. Lattanzio, Publ. Astron. Soc. Aust., **31**, e030, (2014).
[20] S. Yamada T. Suda, Y. Komiya, M. Aiakawa, and M. Y. Fujimoto, unpublished.